液晶与显示
Chinese Journal of Liquid Crystals and Displays

文章编号:1007-2780(XXXX)XX-0001-14

Ferroelectric nematic liquid crystal sings through piezoelectric effect

CHAKRABORTY Susanta[1], CHEN Kangwei[1], YE Jiayao[1], ZHU Zimo[1], TANG Xingzhou[1*], LI Bingxiang[1,2,3*]

(1. *College of Electronic and Optical Engineering & College of Flexible Electronics (Future Technology), Nanjing University of Posts and Telecommunications, Nanjing* 210023, *China*;
2. *State Key Laboratory of Flexible Electronics (LoFE), Nanjing University of Posts & Telecommunications, Nanjing* 210023, *China*;
3. *National Laboratory of Solid State Microstructures, College of Engineering and Applied Sciences, Nanjing University, Nanjing* 210093, *China*)

Abstract: The electroacoustic effect allows electrical control of acoustic waves through the converse piezoelectric effect, which is intrinsic to non-centrosymmetric materials. Ferroelectric nematic liquid crystals (N_F-LCs) combine fluidity with spontaneous polarization, competing with traditional solid ferroelectrics. Here, we show that a confined ferroelectric nematic liquid crystal exhibits a pronounced electroacoustic response under an alternating electric field. The material emits audible sound only upon entering the ferroelectric nematic phase, with a sharp increase in recorded acoustic amplitude. Fourier analysis reveals the distinct underlying electromechanical coupling: the nonpolar nematic phase produces mainly even harmonics under weak electrostriction effect, whereas the polar N_F phase manifests dominant odd harmonics with a low onset voltage (~2 V), owing to a converse piezoelectric effect. The fundamental harmonic strongly dominates over the second harmonic, indicating a pronounced converse-piezoelectric contribution. The acoustic signal amplitude increases monotonically with cell thickness at a constant electric field, consistent with the piezoelectric displacement relation. The programmable operation is demonstrated by reproducing a melody by modulating the driving frequency over time while maintaining a constant voltage. This study presents fluid ferroelectric nematics as a platform for soft, reconfigurable acoustic transducers and sensors with low driving voltages and high piezoelectric responses.

Key words: Ferroelectric nematic liquid crystal; electro-acoustic effect; harmonics; piezoelectricity; electrostriction

收稿日期:2026-05-25;**修订日期**:2026-06-16.

基金项目:国家重点研发计划(No.2022YFA1405000);国家自然科学基金(No. 62375141);江苏省前沿引领技术基础研究专项(No.BK20243067)

Supported by National Key Research and Development Program of China (No.2022YFA1405000); Natural Science Foundation of China (No.62375141); Natural Science Foundation of Jiangsu Province, Major Project (No.BK20243067)

*通信联系人,E-mail:xztang@njupt.edu.cn;bxli@njupt.edu.cn

基于压电效应铁电向列相液晶的电声响应

CHAKRABORTY Susanta[1], 陈康伟[1], 叶家耀[1],
朱子墨[1], 汤星舟[1*], 李炳祥[1,2,3*]
(1. 南京邮电大学 电子与光学工程学院、柔性电子(未来技术)学院, 江苏 南京 210023;
2. 南京邮电大学 柔性电子全国重点实验室, 江苏 南京 210023;
3. 南京大学 固体微结构物理国家重点实验室 现代工程与应用科学学院,
江苏 南京 210093)

摘要:非中心对称材料可通过逆压电效应对声波进行电调控。铁电向列相液晶(N_F-LCs)兼具流动性和可与传统固体铁电体媲美的自发极化特性。本文成功地通过交变电场驱动铁电向列相液晶高效、可编程地发出声音。实验发现其仅在相变为铁电向列相后才会在电场的刺激下发出声音,并伴随有音量的急剧升高。进一步的傅里叶分析揭示了背后独特的底层机电耦合机制:非极性向列相在弱电致伸缩效应下几乎只产生偶次谐波;而极性铁电向列相由于逆压电效应,在低电压(~2LCs)兼具流动性和可与~2 V)下表现出奇次谐波主导,其中基波相对于二次谐波的显著主导表明了明显的逆压电效应存在。在恒定电场下,声音振幅随液晶盒厚度单调递增,与压电位移关系一致。器件的可编程能力通过在恒定电压下随时间调节驱动频率重现一段旋律而得到验证。本研究表明,具备低驱动电压和巨压电响应的铁电向列相流体可用作柔性、可重构的声换能器与传感器平台。

关 键 词:铁电向列相液晶;电声效应;谐波;压电性;电致伸缩
中图分类号:O753$^+$.2 **文献标识码**:A **doi**:10.37188/CJLCD.2026-0093 **CSTR**:32172.14.CJLCD.2026-0093

1 Introduction

The recent discovery of the ferroelectric nematic liquid crystal (N_F-LC) has fundamentally altered the understanding of fluid matter, revealing a state that combines fluidity with spontaneous electric polarization magnitudes comparable to solid-state ferroelectrics[1-7]. Unlike conventional nematic liquid crystals, they are characterized by long-range alignment of directors n along the molecular long axis and breaking of inversion symmetry ($+\boldsymbol{n} \neq -\boldsymbol{n}$), which leads to a macroscopic spontaneous polarization ($\boldsymbol{P}$) that defines a preferred direction parallel to $\boldsymbol{n}$[8-9]. The extraordinary responsiveness of $\boldsymbol{P}$ to a very weak electric field reveals the significant potential of N_F-LCs to be exploited for advancing tunable and faster electromechanical devices. The realization of technological applications of standard nematic liquid crystals was governed by their anisotropic birefringence, dielectric properties, and significant response of the aligned director to an electric field. However, coupled with low viscosity and high fluidity, the remarkable properties of N_F-LCs, like exceptionally large spontaneous polarizations (~5-6 μC/cm^2)[2-3], giant dielectric constants[2,10-11], and strong piezoelectric coefficients[12-13], give rise to novel phenomena, including striking electro-hydrodynamic phenomena, remarkable electro-optic and nonlinear optical effects, piezoelectricity, mechanoelectrical response and dielectrowetting at ultralow voltages[2,12-14], opening unprecedented opportunities for electric field-controlled phenomena that are inaccessible in either material class alone.

The piezoelectricity is mainly influenced by linear coupling between mechanical stress and electric polarization, which is allowed by symmetry[15-16]. Specifically, a shear or splay deformation of a non-centrosymmetric macroscopic arrangement of molecular dipoles tilts the polarization orientation, generating a gradient of bound charge density that manifests as an effective piezoelectric

polarization[17]. Therefore, the N_F-LCs are expected and experimentally confirmed[12,14] to have an intrinsic piezoelectric effect, a property rarely encountered in standard nematics and fluid media, where the directional electromechanical coupling typically averages out. Conversely, an applied electric field exerts a torque on the polarization, induces director reorientation and thereby produces a mechanical strain or stress, defined as the converse piezoelectric effect, which is the physical foundation for several technologies. This unique appearance of linear piezoelectricity in a fluid N_F-LC medium leads directly to a powerful electroacoustic phenomenon, which has recently been observed by Máthé et al. [12-13]. Upon applying an alternating electric field, the periodic torque acting on the polarization induces oscillatory director reorientation. This macroscopic field-induced reorientation of the continuum director field generates propagating mechanical waves via the fluid's viscoelastic stresses. Earlier reports demonstrate direct and converse piezoelectric responses in fluid ferroelectric materials[12], corresponding to strain-induced polarization current and applied-voltage-induced strain, respectively. The observed piezoelectric coupling constant is found to be larger than 1 nC/N, comparable to solid piezoelectric materials. However, theoretical considerations based on symmetry and spontaneous polarization[15-16] suggest that the piezoelectric coefficient should increase with polarization; a perfectly aligned monodomain or absolute homeotropic alignment would therefore yield a larger value than the ~ 1 nC/N reported in unaligned cells[12]. Further, the subsequent work on electrically activated ferroelectric nematic droplet bridges[13] by the same group provided a compelling phenomenological demonstration of electric-field-induced interfacial instabilities and sound generation in these systems, where the motion of fluid bridges accompanied by sound emission is a consequence of piezoelectricity and electrostriction. However, several intrinsic characteristics of electroacoustic transduction, such as the phase-specific nature, its spectral composition, and the role of geometric confinement, remain largely unexplored.

Here, we exploit the direct electro-acoustic transduction in the ferroelectric nematic liquid crystal material DIO, confined in unaligned ITO-coated cells. We show that during the cooling of N_F-LC material, it functions as an exceptionally pronounced acoustic transmitter only in the ferroelectric nematic phase when driven by an AC voltage of lower amplitude (~ 2 V). By systematically varying the frequency, amplitude, and waveform of the driving field, we investigated the characteristics of harmonics of electromechanical response and identified the dominant piezoelectric contributions. The acoustic emission reveals clear phase-dependent behavior, distinguishing the N_F phase from the nematic (N) phase. Additionally, the influence of cell thickness exhibits a direct, monotonic increase in the emitted sound intensity with increasing cell thickness, as explained in detail. Beyond establishing the fundamental physics of electro-acoustic coupling in polar fluids, these results uncover a complex, nonlinear electroacoustic response in ferroelectric nematics that is highly sensitive to phase, confinement, and surface boundary conditions. These findings realize the ferroelectric nematic as a promising soft material platform for potential implications in tunable ultrasound sources, flexible acoustic devices, and novel sensors that harness the extraordinary sensitivity of the ferroelectric nematic phase.

2 Experimental

The ferroelectric nematic liquid crystal (N_F-LC), 2,3',4',5'-tetrafluoro-[1,1'-biphenyl]-4-yl 2,6-difluoro-4-(5-propyl-1,3-dioxan-2-yl) benzoate (DIO), was procured from Nanjing Shuxin Technology Co., Ltd. Fig. 1a illustrates the chemical structure of N_F-LC, DIO and associated phase transition temperatures. The LC cells were

fabricated using two ITO-coated glass substrates without any pre-alignment layer. The thickness of the cells was controlled by UV-curable glue mixed with silica spheres of different diameters and applied to bond two ITO-coated substrates. N_F-LC sample DIO was filled within the cells using capillary action in the high-temperature N phase. The phase sequence and transition temperatures

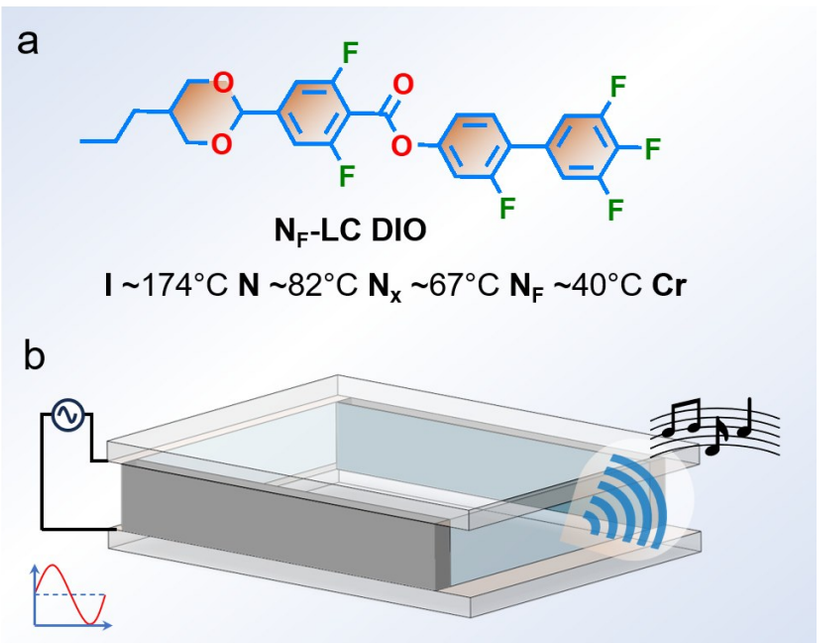

Fig. 1 (a) Molecular structure of N_F-LC DIO and (b) schematic representation of a filled cell for the generation of electro-acoustic effect. The waveform of applied voltage is shown in the bottom left.

were identified by POM textures, in which the N_F transition was indicated by the sudden appearance of multidomain polar textures and the enhanced acoustic response. As shown in Fig. 1b, a sinusoidal AC electric field was applied to the ITO-coated cells of different thickness (~3, 9, 12 and 21 μm). The temperature of the sample was maintained by placing the cell on a hot stage (HCS-402, INSTEC) and controlled by a temperature controller (mk2000B, INSTEC). The cooling rate during acoustic measurements was 1 ℃/min, with temperature stability ±0.1 ℃. The electric field was applied from the function generator (AFG1022, Tektronix) connected to an amplifier (ATA-2041, Xian Aigtek Electronic Technology Co., Ltd.). Optical textures were observed under polarized light using a polarizing optical microscope (Soptop, CX40P). Audio signals were recorded with a smartphone-controlled application Rec Forge II. The built-in microphone of the smartphone was positioned perpendicular to the cell surface at a distance of 1.0 cm. The gain was fixed at 50% (constant amplification and disabling automatic gain control). The recording was saved as 44.1 kHz, 16-bit WAV. Background noise (electric field off) was recorded as −70 dB relative, which was at least 10 dB below the weakest signal (−60 dB). All dB values reported in this manuscript are relative to the full scale of the phone's analog-to-digital converter (0 dB = full scale). No absolute calibration to sound pressure level (dB SPL) was performed. FFT analysis was performed in MATLAB using a Hanning window. The same phone, app, gain, distance, and orientation were used for all measurements, allowing direct internal comparison. However, the uncalibrated nature of this setup precludes comparison with absolute acoustic data from other stud-

ies. All other materials and devices not explicitly mentioned were obtained from local sources.

3 Results and Discussion

3.1 Optical Textures and Electric-Field-Induced Defect Patterns

The ferroelectric nematic liquid crystal (N_F-LC), DIO, was filled into unaligned glass cells of different thicknesses (~3, 9, 12, and 21 μm). Immediately after filling and during cooling from the isotropic state (I), the unaligned sample exhibits non-uniform birefringence textures of the nematic (N) phase through a polarizing optical microscope (POM) with crossed polarizers, which appear black when an electric field is applied, indicating molecular reorientation along the direction of the field. Removing the electric field returns a similar non-uniform texture. Further cooling the sample demonstrates a transition to the intermediate N_X phase (also termed M_2, N_s, or SmZ_A)[18-19], followed by the transition to ferroelectric nematic (N_F) phase at 67 ℃ temperature. This phase transition temperature was identified by observing the crossed polarized POM textures as it cooled at a rate of 1 ℃/min. The transition is marked by the abrupt appearance of a characteristic, strongly birefringent multidomain texture.

Notably, the electric field-induced texture in this N_F phase is completely dependent on the cell thickness. As illustrated in Fig. 2a for a thickness of $d \approx 3$ μm, the applied electric field beyond the onset voltage ($U \approx 1.5$ V) produces a periodic square lattice pattern formed by ±1 defects, simi-

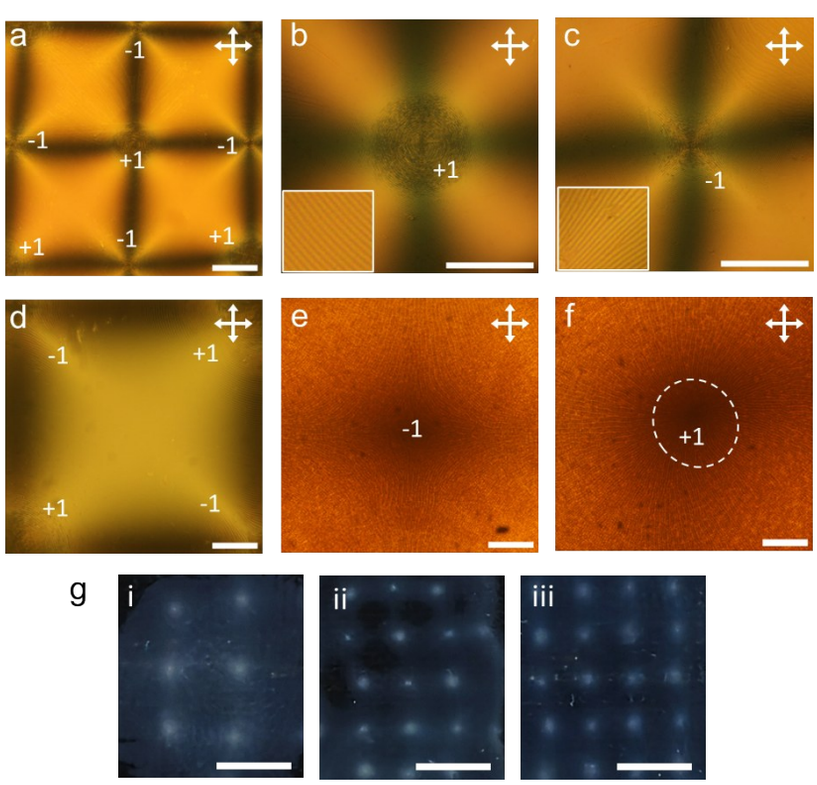

Fig. 2 Polarizing optical textures with crossed polarizers while applying an AC electric field ($U = 10$ V, $f = 3$ kHz, $T = 60$ ℃) to the N_F phase of DIO filled in (a-c) $d \approx 3$ μm, (d) $d \approx 9$ μm and (e, f) $d \approx 21$ μm thick cells. The induced periodic ±1 defects are marked in respective positions in the figure. Crossed white arrows indicate both polarizer directions. (g) Photographs of the entire cell for thickness (i) $d \approx 21$ μm, (ii) $d \approx 12$ μm and (iii) $d \approx 9$ μm cells, under ambient light (no polarizers) with the same applied electric field conditions. The square lattice pattern is visible to the naked eye. Scale bars in (a-f) are of 400 μm and in (g) are of 4 mm.

lar to the earlier reports[20-21]. It is important to note that there are periodic concentric circles centered about +1 defects and also periodic parabolic stripes near −1 defects are observed as shown in Fig. 2b,c and their insets. Since the N_F-LCs produce bound electric charges in response to an applied electric field, at a moderate voltage, the oscillating polarization experiences a stationary interplay between splay and bend, forming a periodic square lattice of ±1 defects[20]. However, for the unaligned surface condition, a recent report[21] confirms that unrestricted polarization couples with the electric field-induced elastic distortions, giving rise to these concentric circles and stripes. Similar observations were also identified for higher thickness cells (≈ 9 μm in Fig. 2d and ≈ 21 μm in Fig. 2e,f). However, with increasing the thickness, the periodicity of the lattice pattern increases, making the pattern hardly visible in a microscope, although visible in the entire cell. Fig. 2g (i-iii) shows photographs of the periodic lattice pattern across the entire electrode area under ambient light (no polarizers) for thicknesses of 21, 12 and 9 μm, respectively. This square lattice pattern is visible across different combinations of amplitude and frequency of applied voltage, although the secondary circular or parabolic stripes are strictly dependent on the frequency of the applied voltage. These secondary patterns smoothly arise when the frequency is about 2 kHz, but with increasing frequency, the periodicity decreases, and both the square lattice and the stripes pattern become distorted and unstable at a frequency above 8 kHz, which makes the cell more unclear, leading to a sharp decrease in transmittance. Remarkably, a pronounced, audible sound appears from the cell in the same frequency range (from 2 kHz to 15 kHz) while these field-induced textures happen, which is quite interesting to explore in this study. Notably, unaligned cells were chosen in this study to avoid preferential polarization orientation, allowing the field-induced formation of periodic defect lattices (Fig. 2g) and maximizing the effective piezoelectric response by minimizing surface-imposed polarization suppression.

3.2 Electroacoustic Response and Influence of Different Parameters

To investigate the electroacoustic effect, we utilized a cell of thickness $d \approx 21$ μm and cooled down the sample from the isotropic state (I) under a sinusoidal AC electric field (frequency $f_{App} = 3$ kHz and amplitude $U = 10$ V), which is well above the onset voltage both in nematic (N) and ferroelectric nematic (N_F) phases. The reported acoustic level is a relative amplitude extracted from the microphone signal and is not calibrated as an absolute sound pressure level. As shown in Fig. 3a, the sound level in the N and intermediate N_X phases is almost constant at about −60 dB. However, upon entering the N_F phase at ~67 ℃, the sound level follows a sharp increase and gradually saturates at −27 dB, ensuring a measurable electromechanical response when the material transforms polar. Notably, no distinct acoustic step is observed for the N_X phase, confirming that the electroacoustic response only differentiates the polar N_F phase from the non-polar N and N_X phases. The change in optical texture and associated acoustic signal is provided in supplementary video S1. This noticeable increase is a strong indication of the converse piezoelectric effect, which is forbidden in the centrosymmetric N phase but emerges with the spontaneous polarization ($\boldsymbol{P}_s$) in the N_F phase. The conventional nematic phase, possessing head-tail symmetry, prohibits linear electromechanical coupling. Consequently, the quadratic effects such as electrostriction are allowed, producing mechanical strain at twice the driving frequency ($2f_{App}$). Therefore, the constant low sound level in the N and N_X phases is attributed to electrostriction, which is quadratically coupled to the field and typically produces a smaller strain than the linear piezoelectric effect at low voltages. In contrast, the polar N_F phase has $C_{\infty v}$ symmetry,

which lacks the mirror inversion symmetry, and permits non-zero piezoelectric tensor elements[12]. The linear coupling between the applied electric field and mechanical strain generates a strong acoustic emission at the fundamental frequency $f_{App,}$ leading to the observed increase in sound level. Since the piezoelectric coupling constant scales with P_s, the sound level increases and saturates when the polarization reaches its maximum. A recent report demonstrates that the direct mechano-electric response in the N_F-LC sample exists only in the N_F phase[14]. Our converse electroacoustic measurement supports that fluid polar order is crucial for any linear electromechanical or mechano-electrical response.

The Fourier analysis of this acoustic signal, both in the N and N_F phases, was performed, which provides essential evidence for electromechanical coupling. Fig. 3b shows that under the electric field of frequency $f_{App} = 5$ kHz and amplitude $U = 60$ V, the N phase represents only even harmonics ($2f_{App}$, $4f_{App}$, and so on) of the FFT signal, where the second harmonic is dominant. Therefore, only even-order harmonics in the N phase resemble the characteristic signature of electrostriction because it does not require broken inversion symmetry. Even order harmonics are also observed with a lower amplitude of the applied electric field, which becomes pronounced with increasing amplitude. Conversely, in the N_F phase (Fig. 3c), with the electric field of frequency $f_{App} = 5$ kHz and a smaller amplitude $U = 10$ V, in addition to the even harmonics, dominant odd harmonics are also present, indicating the converse piezoelectric effect, agreed with the earlier report[13]. The coexistence of harmonics at both f_{App} and $2f_{App}$ signifies that electrostriction is still acting, but superimposed on a much stronger piezoelectric response, even with a much lower amplitude of applied voltage. Note that a control experiment with conventional non-ferroelectric nematic liquid crystal (5CB) produced only weak even harmonics due to electrostriction, confirming that the strong odd-harmonic response is unique to the N_F phase. At a fixed temperature and fixed applied voltage, the amplitudes of the harmonics at both f_{App} and $2f_{App}$ vary with the driving frequency. The frequency dependence of FFT signals is shown in Fig. 3d, e for N and N_F phases, respectively, in which it is clear that the amplitudes (A_{FFT}) of second harmonics (H_2) in the N phase and A_{FFT} of first harmonics (H_1) in N_F phases are dominated irrespective of the frequency beyond 2 kHz. Note that this study is limited to a frequency range of 1～10 kHz, because at lower frequencies than 1 kHz, the response is often dominated by viscous flow[14].

Since we are mostly interested in the electroacoustic effect in the N_F phase, a comparative variation of A_{FFT} for H_1 and H_2 with respect to frequency is shown in Fig. 4a. It is clear that at a constant temperature of 60 ℃ and voltage of 10 V, A_{FFT} for H_1 and H_2 increases with the frequency of the driving field. Notably, below approximately 5 kHz, A_{FFT} for H_2 dominates, while in the frequency region above 5 kHz, the same for H_1 becomes larger. This behavior reflects the interplay between electrostriction and the converse piezoelectric effect. The crossover from H_2-dominated to H_1-dominated response around several kilohertz suggests a change in the relative interplay between nonlinear electrostrictive processes and polar linear electromechanical coupling. Possible factors include ionic screening, viscous director relaxation, field-induced texture reconfiguration, and the frequency-driven acoustic response of the cell substrate. A quantitative separation of these contributions would require phase-resolved measurements and impedance/acoustic calibration, which are beyond the scope of the present study. Máthé et al. [12] reported that the linear electromechanical response in two different N_F-LCs was strongest in the range 3～6 kHz, with the first harmonic amplitude increasing with frequency up to a maximum

and then decreasing. Our frequency dependence shares the same general feature that the polar N_F phase supports a strong first-harmonic electromechanical response[12], but the detailed frequency dependence differs from previous measurements[13]. This dissimilarity arises probably due to the difference in material geometry, i. e., the present study deals with a confined ITO cell rather than a moving droplet or liquid bridge. Additionally, the acoustic output is also affected by boundary conditions, active volume, surface anchoring, and cell mechanics. However, it is also found that deep in the N_F phase, the piezoelectric coupling remains significant across the measured frequency range (2～10 kHz), although its relative strength compared to electrostriction varies with frequen-

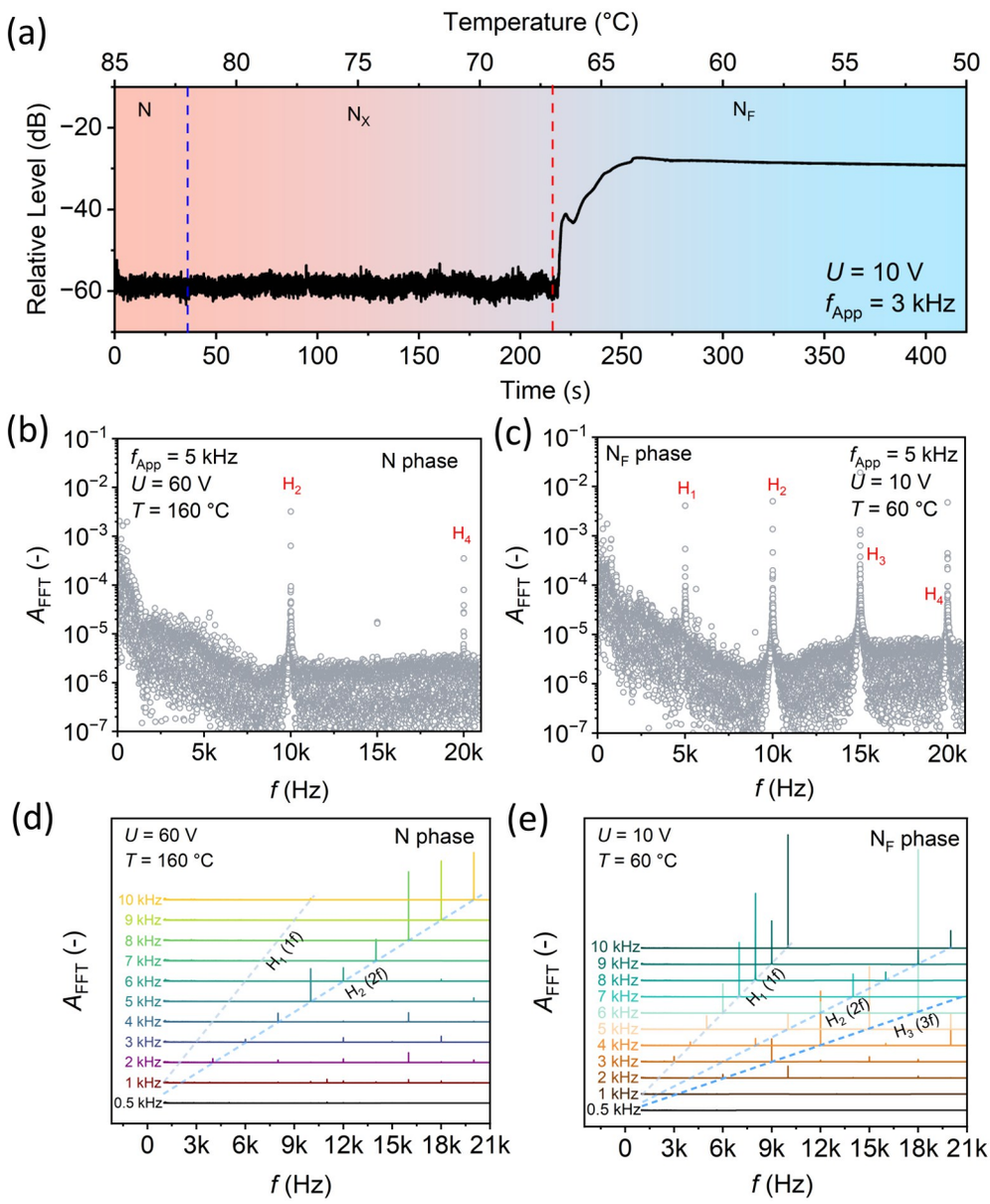

Fig. 3 Parameters of the electroacoustic response in N and N_F phases. (a) Measured sound level of the unaligned N_F-LC (d ~21 μm) during cooling under an electric field (f_{App} = 3 kHz, U = 10 V). Vertical dashed lines are the transition temperatures of consecutive phases. Fourier signal of emitted sound in (b) N phase with f_{App} = 5 kHz, U = 60 V and (c) N_F phase with f_{App} = 5 kHz, U = 10 V. Variation of FFT amplitudes with frequency in (d) N phase with U = 60 V and (e) N_F phase with U = 10 V. Orders of harmonics are labeled in respective figures.

cy. Fig. 4b illustrates the variation of A_{FFT} with the amplitude of voltage at a constant frequency of 6 kHz. Here, both the H_1 and H_2 amplitudes exhibit an onset voltage of approximately ~2 V. Further increasing the voltage, both components rise progressively, while the H_1 amplitudes are always higher than the H_2 amplitudes. The finite onset voltage indicates that the measured acoustic emission is not a purely small-signal piezoelectric response. Instead, it likely involves polar director reconfiguration, domain rearrangement, and field-induced defect or texture evolution in the confined N_F cell. Above this onset, the strong H_1 component suggests that the polar phase enables a linear electromechanical contribution. In contrast, the nematic phase shows only H_2 component, with a much higher onset voltage (>10 V) and a very slow increase with voltage, supporting the absence of piezoelectricity in the non-polar phase[12].

Further observation with variation in temperature (Fig. 4c) confirms that as the temperature decreases through the transition to N_F phase (≈ 67 ℃), both the H_1 and H_2 amplitudes sharply grow, with the H_1 amplitude exceeding the H_2 component. This again suggests that the emergence and growth of spontaneous polarization enable the linear piezoelectric effect and it is the primary property for the transduction mechanism. All the studies discussed above were obtained due to the applied AC electric field having a sinusoidal waveform. To quantitatively separate the piezoelectric and electrostrictive contributions from Fig. 4b, we exploit the quadratic scaling of electrostriction, where H_2 amplitude scales with the square of E ($\propto E^2$). In the non-polar N phase, where piezoelectricity is absent, H_2 arises purely from electrostriction (U=60 V, $A_{FFT}\approx 5\times10^{-3}$, relative units). Scaling this to 10 V in the N_F

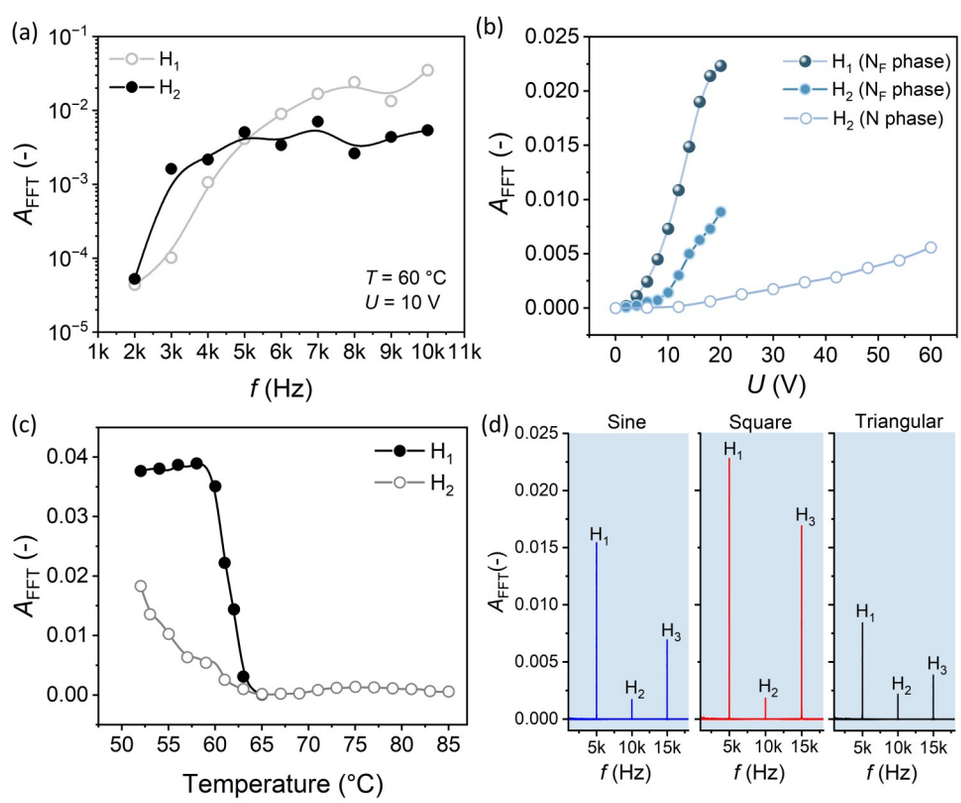

Fig. 4 Extracted amplitude (A_{FFT}) from Fourier analysis of the electro-acoustic response with variation of (a) frequency, (b) voltage of applied electric field and (c) temperature of the sample. (d) Variation of A_{FFT} for applying the electric field of different waveforms, maintaining the same frequency and voltage.

phase, the expected A_{FFT} amplitude for H_2 would be $A_{FFT}(N_F) = A_{FFT}(N) \times (10/60)^2 \approx 1.4 \times 10^{-4}$. However, the experimentally obtained value of A_{FFT} in the N_F phase at $U = 10$ V (from Fig. 4b) is $\approx 1.3 \times 10^{-3}$ (relative unit), indicating an enhanced electrostrictive coefficient in the polar N_F phase or a minor nonlinear piezoelectric contribution. Conversely, the purely piezoelectric H_1 amplitude in the N_F phase at 10 V is 7.3×10^{-3} (Fig. 4b), which is approximately 50 times larger than the pure electrostrictive baseline. This quantitative analysis confirms that the converse piezoelectric effect dominates the electroacoustic response in the N_F phase.

In contrast, it is interesting to study the influence of the electroacoustic response with different waveforms. Fig. 4d exhibits the comparative variation of A_{FFT} for electric field ($f_{App} = 5$ kHz, $U = 9$ V) having sinusoidal, square and triangular waveforms at a sample temperature 55 ℃. The electroacoustic response depends strongly on the applied voltage waveform: the square wave produces the largest signal, followed by the sine wave, then the triangular wave. Ideally, a square wave contains a large fundamental amplitude and strong odd harmonics, efficiently driving both the piezoelectric and electrostriction responses, while the triangular wave has lower fundamental content and a negligible second harmonic component in the ideal case. However, we observed that the use of a square waveform induces the possibility of making air traps inside the sample cell, which degrades the material property and modifies the sound level. Due to a sudden change or turn off in the electric field, Máthé et al. also observed the splitting of droplets into parts[13]. Therefore, we have restricted this study to use the electric field with only a sinusoidal waveform.

Further attempt to study the influence of sample thickness on the acoustic response, we systematically measured the temperature-dependent acoustic response by varying the cell thickness $d \sim 9$, 12 and 21 μm cells while keeping a constant frequency $f_{App} = 6$ kHz and constant electric field ($E = U/d = 0.83$ V/μm) as shown in Fig. 5a. Below the transition to N_F phase, the audio signal emerges and strengthens from a temperature ≈ 65 ℃ for all thicknesses, but the sound intensity increases monotonically with cell thickness. FFT analysis shows that the amplitude A_{FFT} for both H_1 and H_2 components enhances with thickness (Fig. 5b). For a fixed field, the piezoelectric displacement scales as $\Delta z = \gamma_{z,zz}. E. d$, where E is the electric field and d is the thickness of material[12]. So, a thicker cell produces a larger mechanical amplitude and thus higher recorded acoustic amplitude. Additionally, the total active volume increases with d, leading to greater radiated acoustic power. In a very thin cell, the entire thickness is within the surface-dominated region, and the polarization tilt is suppressed. The surface-confined region in a thicker cell occupies a smaller fraction of the total thickness, so the bulk polarization is effectively decoupled from the surface anchoring forces. Since the electric field is identical, the thicker cell allows a larger net polarization tilt because of relatively weaker surface-imposed constraints. This effect is analyzed by Basnet et al. [20] for the splay Fréedericksz transition, where the onset for stationary deformations depends on the ratio between thickness and characteristic length for splay deformation. The piezoelectric coefficient is largest when polarization or its significant components are aligned with the field. Therefore, a thicker cell reaches a higher effective piezoelectric coefficient for the same electric field, leading to a stronger acoustic emission, as expected from the piezoelectric constitutive relation. Moreover, the frequency dependence of H_1 in Fig. 5c follows the same increasing pattern irrespective of cell thickness, though above 4 kHz, thicker cells exhibit a substantially larger A_{FFT} amplitude. This suggests that at high frequencies, reduced viscous dissipation prevents the flow from fully developing across

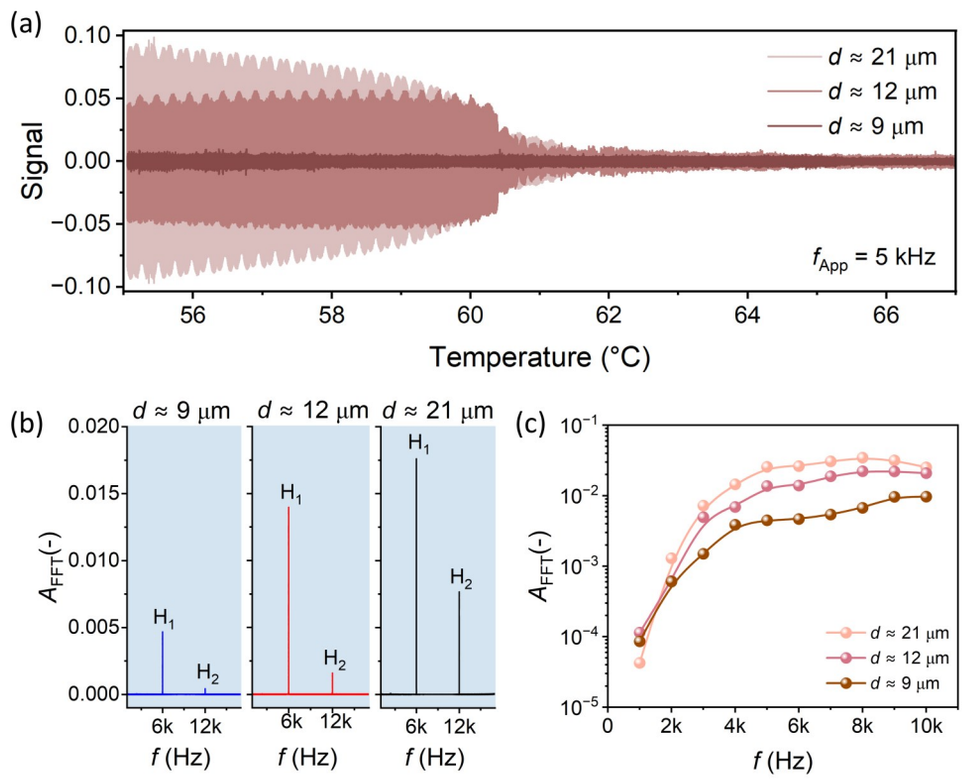

Fig. 5 (a) Temperature dependence of the electroacoustic signal for cells of thickness d = 9 μm, 12 μm, and 21 μm. The measurements were performed at a constant electric field E = 0.83 V/μm and f_{App} = 6 kHz) (b) A_{FFT} amplitude for three cell thicknesses at constant field and temperature (60 ℃) and (c) Frequency variation of H_1 amplitude for three cell thicknesses.

the thicker layer. To ensure reproducibility, measurements were repeated on at least two independently fabricated cells for each thickness. The observed trends were almost consistent across cells of similar thickness. The data shown in the figures are representative of these repeated measurements.

Collectively, the results presented above establish that ferroelectric nematic liquid crystals exhibit a robust, tunable, and scalable converse piezoelectric effect in the fluid state. The sharp increase in sound emission on entering the N_F phase, the dominance of the fundamental harmonic (H_1) over the second harmonic (H_2), the linear voltage dependence, and the enhancement with cell thickness all confirm that the electromechanical coupling is predominantly realized in the giant piezoelectric and intrinsic to the polar phase. To translate these fundamental insights into dynamic programmability of the electroacoustic response, we encoded the melody of "Happy Birthday to You" by varying the frequency of the applied AC electric field in a definite time sequence while keeping the voltage constant (Supplementary video S2). Fig. 6a presents the variation of applied frequency as a function of time, along with the corresponding audio signal and its spectrogram, showing the frequency content over time are depicted in Fig. 6b and c, respectively. The applied frequency pattern follows the note sequence of the melody, and the recorded sound reproduces the expected pitch variations. The spectrogram confirms that the dominant frequency components match the applied frequencies, with minimal harmonic distortion. This proof-of-concept experiment shows that the acoustic pitch can be modulated in real time by changing the driving frequency, allowing the N_F-LC cell to reproduce a simple melody under constant voltage. Beyond the musical

analogy, this capability may have practical implications for acoustic labeling, temperature sensors, non-contact signaling, and tunable sound sources in microfluidic or soft robotics applications, tunable alarms or identifiers in flexible electronics, and fluid-based piezoelectric actuators that can be integrated into wearable or biomedical devices. Thus, our work not only advances the fundamental understanding of electromechanics in fluid ferroelectrics but also opens a pathway toward a new class of reconfigurable, soft, and liquid-based acoustic transducers.

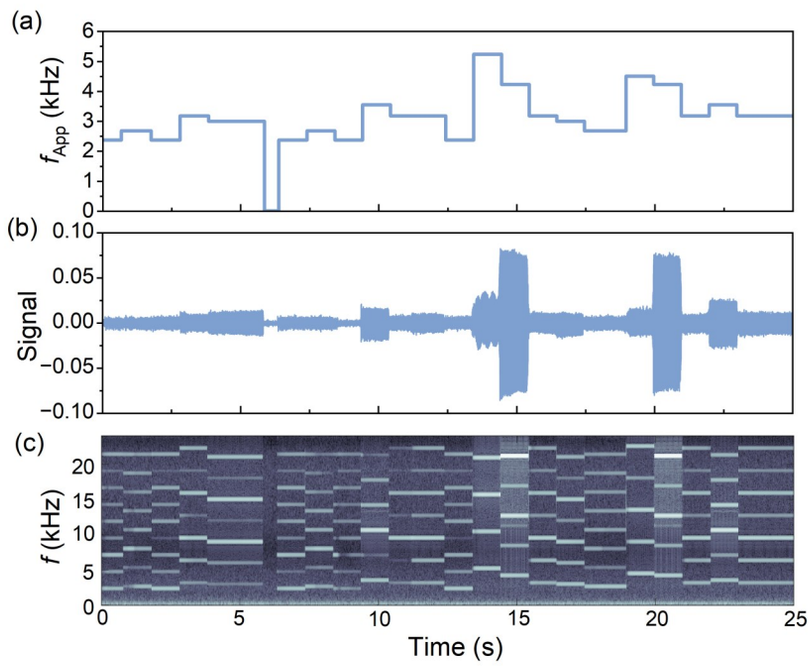

Fig. 6 Programmable acoustic signal generation by frequency modulation. (a) Applied frequency as a function of time, at constant voltage $U = 10$ V. (b) Corresponding recorded audio signal from the 21 μm cell. (c) Spectrogram of the audio signal, showing frequency components of harmonics.

4 Conclusion

This study establishes that a ferroelectric nematic liquid crystal (N_F-LC) confined in an unaligned cell exhibits a pronounced, tunable, and phase-specific electroacoustic response. The sound emission occurs only in the N_F phase, with a sharp increase of 33 dB at the transition, with a very low electric field. Fourier analysis shows that the non-polar nematic phase produces mainly even harmonics due to electrostriction, whereas the polar ferroelectric phase generates both odd and even harmonics, supporting a strong converse piezoelectric effect. The dominance of odd harmonics above 4 kHz appears above an onset voltage of approximately 2 V and increases progressively with voltage. Together, the phase-dependent enhancement of the acoustic signal, the emergence of a strong first-harmonic component in the N_F phase, and the thickness-dependent output support the interpretation that polar electromechanical coupling plays a major role in the electroacoustic response of confined ferroelectric nematic liquid crystals. The coexistence of H_1 and H_2 components further indicates that converse-piezoelectric-like and electrostrictive contributions are both present. An effective interplay between unrestricted polarization and electric field-induced viscoelastic distortions

plays a crucial role in dominating the fundamental piezoelectricity over electrostriction. The acoustic output depends on driving frequency, voltage, waveform, temperature, and cell thickness, indicating that both material properties and confinement geometry are important. Finally, frequency modulation of the driving voltage enables the cell to reproduce a simple melody, demonstrating a proof-of-concept route toward frequency-programmable soft electroacoustic elements. This study is limited to only N_F-LC material, DIO and unaligned cells. Future investigations using aligned monodomains and calibrated acoustic measurements will be necessary to enable quantitative determination and comparison of the piezoelectric coefficient with theory and to assess the generalizability of the observed electroacoustic behavior. Beyond establishing the fundamental physics of electroacoustic transduction in polar soft matter, these findings position ferroelectric nematic liquids as a versatile material platform for a new class of reconfigurable, fluid-based acoustic transducers, sensors and actuators with potential applications in soft robotics and wearable electronics.

References:

[1] Mandle R J, Cowling S J, Goodby J W. A nematic to nematic transformation exhibited by a rod-like liquid crystal. [J]. *Phys. Chem. Chem. Phys.* 2017, 19 (1): 11429-11435.

[2] Nishikawa H, Shiroshita K, Higuchi H, *et al*. A fluid liquid-crystal material with highly polar order. [J]. *Adv. Mater.* 2017, 29 (43): 1702354.

[3] Chen X, Korblova E, Dong D, *et al*. First-principles experimental demonstration of ferroelectricity in a thermotropic nematic liquid crystal: Polar domains and striking electro-optics. [J]. *Proc. Natl. Acad. Sci.*, 2020, 117 (25): 14021-14031.

[4] Mandle R J, Sebastián N, Martinez-Perdiguero J, *et al*. On the molecular origins of the ferroelectric splay nematic phase. [J]. *Nat. Commun.*, 2021, 12: 4962.

[5] Gibb C J, Mandle R J. New RM734-like fluid ferroelectrics enabled through a simplified protecting group free synthesis. [J]. *J. Mater. Chem. C*, 2023, 11:16982-16991.

[6] Mandle R J. A new order of liquids: Polar order in nematic liquid crystals. [J]. *Soft Matter*, 2022, 18 (27): 5014-5020.

[7] Lavrentovich M O, Lavrentovich P K, Lavrentovich O D. Twist, splay, and uniform domains in ferroelectric nematic liquid crystals. [J]. *Nat. Commun.*, 2024, 16: 6516.

[8] Chen X, Korblova E, Glaser M A, *et al*. Polar in-plane surface orientation of a ferroelectric nematic liquid crystal: Polar monodomains and twisted state electro-optics. [J]. *Proc. Natl. Acad. Sci.*, 2021, 118 (31): e2104092118.

[9] Rudquist P. Revealing the polar nature of a ferroelectric nematic by means of circular alignment. [J]. *Sci. Rep.*, 2021, 11: 24411.

[10] Clark N A, Chen X, MacLennan J E, *et al*. Dielectric spectroscopy of ferroelectric nematic liquid crystals: Measuring the capacitance of insulating interfacial layers. [J]. *Phys. Rev. Res.*, 2024, 6 (1): 013195.

[11] Vaupotič N, Pociecha D, Gorecka E, *et al*. Dielectric response of a ferroelectric nematic liquid crystalline phase in thin cells. [J]. *Liq. Cryst.*, 2023, 50 (3): 584-595.

[12] Máthé M T, Himel M S H, Adaka A, *et al*. Liquid piezoelectric materials: Linear electromechanical effect in fluid ferroelectric nematic liquid crystals. [J]. *Adv. Funct. Mater.*, 2024, 34 (18): 2314158.

[13] Máthé M T, Nishikawa H, Araoka F, *et al*. Electrically activated ferroelectric nematic microrobots. [J]. *Nat. Commun.*, 2024, 15: 6928.

[14] Medle Rupnik P, Cmok L, Sebastián N, *et al*. Viscous mechano-electric response of ferroelectric nematic liquid. [J]. *Adv. Funct. Mater.*, 2024, 34 (38): 2402554.

[15] Newnham R E. Properties of Materials: Anisotropy, Symmetry, Structure [M]. Oxford University Press, 2005.

[16] Landau L D, Lifshitz E M. Electrodynamics of Continuous Media, 2nd ed. [M]. Pergamon Press, 1984.

[17] Willatzen M. Piezoelectricity in Classical and Modern Systems [M]. Bristol: IOP Publishing, 2024.
[18] Chen X, Martinez V, Korblova E, *et al*. The smectic Z_A phase: Antiferroelectric smectic order as a prelude to the ferroelectric nematic. [J]. *Proc. Natl. Acad. Sci.*, 2023, 120(6): e2217150120.
[19] Nacke P, Tuffin R, Klasen-Memmer M, *et al*. Revealing the antipolar order in the antiferroelectric SmZ_A phase by means of circular alignment. [J]. *Sci. Rep.*, 2024, 14: 15018.
[20] Basnet B, Paladugu S, Kurochkin O, *et al*. Periodic splay Fréedericksz transitions in a ferroelectric nematic. [J]. *Nat. Commun.*, 2025, 16: 1444.
[21] Sahoo R, Nagaraj M, Raistrick T, *et al*. Optically selective photomask based on field-induced periodic defect arrays in ferroelectric nematics. [J]. *Adv. Opt. Mater.*, 2026, 14: e03769.

作者简介：

Susanta Chakraborty received his Ph. D. degree from University of North Bengal, India, in 2019. Following this, he worked at the Indian Institute of Technology Delhi, India, from 2019—2024. Currently, he is working at Nanjing University of Posts and Telecommunications as post-doctorate fellow. His research interests include experimental liquid crystal physics, particularly in electro-optic switching, polymer-based systems, and the development of optical sensors, energy harvesting and electro-optic devices. E-mail: susanta0101@gmail.com

Xing-Zhou. Tang received his Ph. D. degree in Chemical Physics from Advanced Material and Liquid Crystal Institute at Kent State University in 2020. He is currently a professor in Nanjing University of Posts and Telecommunications. His current research spans from liquid crystals, active matter and biological physics. E-mail: xztang@njupt.edu.cn

Bing-Xiang Li. received his Ph. D. degree in Chemical Physics from Advanced Material and Liquid Crystal Institute at Kent State University in 2019. He is currently a professor in Nanjing University of Posts and Telecommunications. His current research spans from liquid crystals, stimuli-responsive soft matter, active matter, to biological physics. E-mail: bxli@njupt.edu.cn